ChemistryOPEN Full Papers

ChemPubSoc Europe

Open Access

DOI: 10.1002/open.201402020

Rhodamine-Appended Bipyridine: XOR and OR Logic Operations Integrated in an Example of Controlled Metal Migration**

Cristina Núñez,*[a, b, c, d] Sergio M. Santos,[e] Elisabete Oliveira,[a, d] Hugo M. Santos,[a, d] José Luis Capelo,[a, d] and Carlos Lodeiro*[a, d]

A new bipyridyl derivative **1** bearing rhodamine B as visible fluorophore was designed, synthesized and characterized as a fluorescent and colorimetric sensor for metal ions. Interaction with Cu^{2+}, Zn^{2+}, Cd^{2+}, Hg^{+}, and Hg^{2+} ions was followed by UV/Vis and emission spectroscopy. Upon addition of these metal ions, different colorimetric and fluorescent responses were observed. "Off-on-off" (Cu^{2+}, Zn^{2+}, and Hg^{2+}) and "off-on" (Hg^{+} and Cd^{2+}) systems were obtained. Probe **1** was explored to mimic XOR and OR logic operations for the simultaneous detection of Hg^{+}–Cu^{2+} and Hg^{+}–Zn^{2+} pairs, respectively. DFT calculations were also performed to gain insight into the lowest-energy gas-phase conformation of free receptor **1** as well as the atomistic details of the coordination modes of the various metal ions.

Introduction

The development of artificial receptors for sensing and recognition of environmentally and biologically important ionic species, especially transition and post-transition metal ions, is currently of great interest in various fields of science as biological probes,[1] environmental sensors,[2] and molecular devices.[3]

Chemistry plays a key role in the controlled design of molecular and supramolecular structures, which can be addressed by external stimuli (input), and which generate one or more answer signals (output). These systems that process input signals by means of combinatorial operations are called logic gates.[4]

A receptor with varying affinities for different metal ions and with multiple coordination modes is expected to execute both simple and integrated logic operations,[5] provided that binding through different coordination modes and to different metal ions is associated with changes in optical output in terms of intensity and wavelength.[6] Various methodologies have been used to achieve the desired modulation in optical output in terms of changes in the fluorescence or absorption spectral properties on binding to certain metal ions. Among these, intramolecular charge transfer (ICT) and photoinduced electron or energy-transfer-based processes have been widely used.[3,7]

Migration of metal ions across polymer membranes in compartmental cyclic ligands is known;[8] however, there are fewer reported examples of site-specific metal ion migration in an acyclic ligand.[9] To the best of our knowledge, Das and coworkers[9] reported the only example in which metal ion migration modulates the absorption and fluorescence response for executing molecular-level logic gates.

Taking into account the advantageous photophysical[10] and sensing properties[11] of rhodamine-based compounds, and our research interest on the design, synthesis, and evaluation of ar-

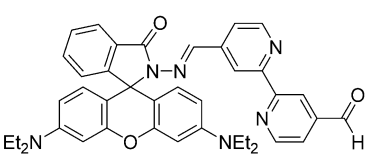

1

[a] Dr. C. Núñez, Dr. E. Oliveira, Dr. H. M. Santos, Prof. Dr. J. L. Capelo, Prof. Dr. C. Lodeiro
BIOSCOPE Group, REQUIMTE
Chemistry Department, Faculty of Science and Technology
University NOVA of Lisbon, 2829-516 Caparica (Portugal)
E-mail: cle@fct.unl.pt
cristina.nunez@fct.unl.pt

[b] Dr. C. Núñez
Inorganic Chemistry Department, Faculty of Chemistry
University of Santiago de Compostela
15782 Santiago de Compostela (Spain)

[c] Dr. C. Núñez
Ecology Research Group, Department of Geographical & Life Sciences
Canterbury Christ Church University, CT1 1QU, Canterbury (UK)

[d] Dr. C. Núñez, Dr. E. Oliveira, Dr. H. M. Santos, Prof. Dr. J. L. Capelo, Prof. Dr. C. Lodeiro
PROTEOMASS Scientific Society
Madan Parque, Rua dos Inventores, 2825-182 Caparica (Portugal)

[e] Dr. S. M. Santos
Department of Chemistry & CICECO, University of Aveiro
Campus de Santiago, 3810-193 Aveiro (Portugal)

[**] This article is part of the Virtual Special Issue "Molecular Sensors"

Supporting information for this article is available on the WWW under http://dx.doi.org/10.1002/open.201402020.

tificial receptors,[12] herein we report a novel bipyridyl derivative **1** bearing rhodamine B to explore its sensing properties toward various metal ions (Cu^{2+}, Zn^{2+}, Cd^{2+}, Hg^{+}, and Hg^{2+}). The spectral response associated with the unusual different migration of the metal ions from the chelating rhodamine terminal in the open-ring form to the remote bipyridyl terminal, leads to a combination of optical responses that could be correlated for demonstrating some simple logic operations.

Results and Discussion

Molecular probe **1** was synthesized by following a one-pot reaction procedure using a 2:1 mixture of rhodamine B hydrazide and 2,2′-bipyridine-4,4′-dicarboxaldehyde in absolute ethanol/tetrahydrofuran (1:1) (Scheme 1).

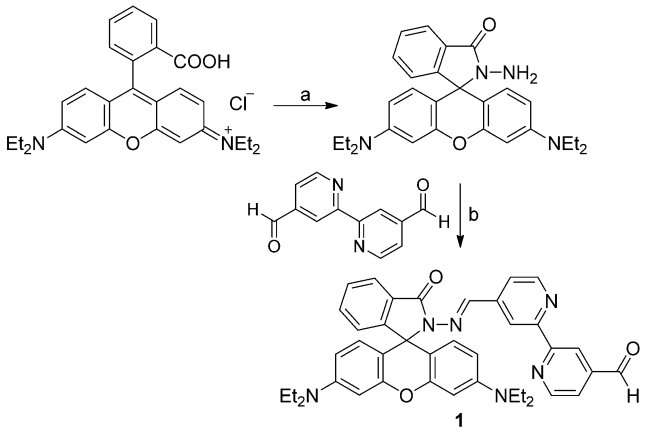

Scheme 1. Synthetic route of compound **1**. *Reagents and conditions*: a) $NH_2NH_2{\cdot}H_2O$, abs. EtOH, reflux, 3 h, 90%; b) abs. EtOH/THF (1:1), reflux, 2 h, 86%.

Spectrophotometric and spectrofluorimetric studies

Owing to the low solubility observed in water for probe **1**, all spectrophotometric measurements were conducted in dichloromethane solution. The absorption spectra of probe **1** in dichloromethane resulted from the sum of two species (bipyridyl and rhodamine groups), showing bands at 220–280 and ~319 nm attributed to the higher-energy ligand-localized π–π^* transitions (see Supporting Information (SI) Figure SI 1). The absorption spectrum of **1** was coincident with the excitation spectrum, which confirms the purity of this compound in solution. Compound **1** did not absorb in the 500–600 nm region; moreover, molecular probe **1** exhibited very weak fluorescence ($\Phi < 0.001$). Both effects indicated that **1** is present in the spirocycle-closed form.

The receptor molecule **1** has two distinctly different binding sites: a rhodamine and a bipyridyl unit. Both moieties are known to bind strongly to several metal ions.

Figure 1 A,C,E shows the absorption spectra of compound **1** in the presence of increasing amounts of Cu^{2+}, Zn^{2+}, and Hg^{2+}, respectively. If no metal ion was added to the solution of **1** (5.0×10^{-6} M) almost no absorption in the 500–600 nm region was observed due to the rhodamine spiro conformation in solution, whereas addition of one equivalent of Cu^{2+}, Zn^{2+}, and Hg^{2+} led to the appearance of strong absorption transitions at ~562–564 nm, with a shoulder at ~518–520 nm, which is characteristic of rhodamine-based dyes.[13]

Upon addition of Cu^{2+} (Figure 1 A), Zn^{2+} (Figure 1 C), and Hg^{2+} (Figure 1 E), a metal-induced lactam cleavage of the rhodamine—from the initial spirolactam form to the ring-opened amide conformation—took place, facilitating complex formation. The subsequent colorless/pink transition in the presence of these metal ions yield significantly high absorptions: $\varepsilon = 3.6\times10^4\ dm^3\,mol^{-1}\,cm^{-1}$ at 562 nm (with Cu^{2+}), $\varepsilon = 3.4\times10^4\ dm^3\,mol^{-1}\,cm^{-1}$ at 562 nm (with Zn^{2+}), and $\varepsilon = 5.0\times10^4\ dm^3\,mol^{-1}\,cm^{-1}$ at 564 nm (with Hg^{2+}).

The fluorescence enhancement effects of Cu^{2+} (Figure 1 B), Zn^{2+} (Figure 1 D), and Hg^{2+} (Figure 1 F) metal ions on receptor **1** were also investigated. Excitation was performed at 520 nm rather than the peaks of the absorption spectrum (~560 nm) to obtain a full view of the fluorescence spectra from 530 to 700 nm. In the absence of Cu^{2+}, Zn^{2+}, and Hg^{2+} metal ions, **1** did not exhibit fluorescence (SI, Figure SI 1). If one equivalent of these metals were introduced to a solution of **1** in dichloromethane, the conversion from the cyclic lactam form to the acyclic xanthene took place, and was associated with an increase in the emission intensity observed. Probe **1** (5.00×10^{-6} M) exhibited 34-fold ($\Phi_{FT} = 0.453$), 31-fold ($\Phi_{FT} = 0.413$), and 43-fold ($\Phi_{FT} = 0.573$) enhancements in fluorescence intensity at peak wavelengths $\lambda_{max} = 577$ nm (Cu^{2+}) and 580 nm (Zn^{2+} and Hg^{2+}) in the presence of one equivalent of each metal ion.

It was observed that the absorbance and fluorescence emission of probe **1** increased to attain the maxima with the addition of one equivalent of Cu^{2+} (Figure 1 A,B), Zn^{2+} (Figure 1 C,D), and Hg^{2+} (Figure 1 E,F) ions. Surprisingly, the subsequent increase in the concentration of metal added leads to a gradual decrease (see insets).

However, the addition of one equivalent or increasing quantities of Hg^{+} (Figure 2 A,B) or Cd^{2+} (Figure 2 C,D) to a dichloromethane solution of compound **1** led to the appearance and the maintenance of strong absorption ($\varepsilon = 7.2\times10^4\ dm^3\,mol^{-1}\,cm^{-1}$ and $\varepsilon = 6.0\times10^4\ dm^3\,mol^{-1}\,cm^{-1}$ at 561 nm with Hg^{+} and Cd^{2+}, respectively) and fluorescence emission bands (52-fold ($\Phi_{FT} = 0.693$) and 48-fold ($\Phi_{FT} = 0.640$) at 579 nm with of Hg^{+} and Cd^{2+}, respectively).

To further investigate the binding mode of **1** with Cu^{2+}, Zn^{2+}, Hg^{2+}, Hg^{+}, and Cd^{2+}, Job's plots were also carried out. In all cases, the data exhibited a maximum absorbance and fluorescence emission when the molecular fraction of **1** was close to 50%, which also suggests a 1:1 stoichiometry for the **1**–Cu^{2+}, **1**–Zn^{2+}, **1**–Hg^{2+}, **1**–Hg^{+} and **1**–Cd^{2+} complexes (see SI, Figure 2 SI).

These results indicate that in the case of Cu^{2+}, Zn^{2+}, and Hg^{2+}, metals initially interact with the molecular probe **1** by coordination with the delocalized amide unit which results in an increase in the absorption and fluorescence emission response. It was then followed by the migration of the metal ions from the amide to the bipyridine framework, yielding a de-

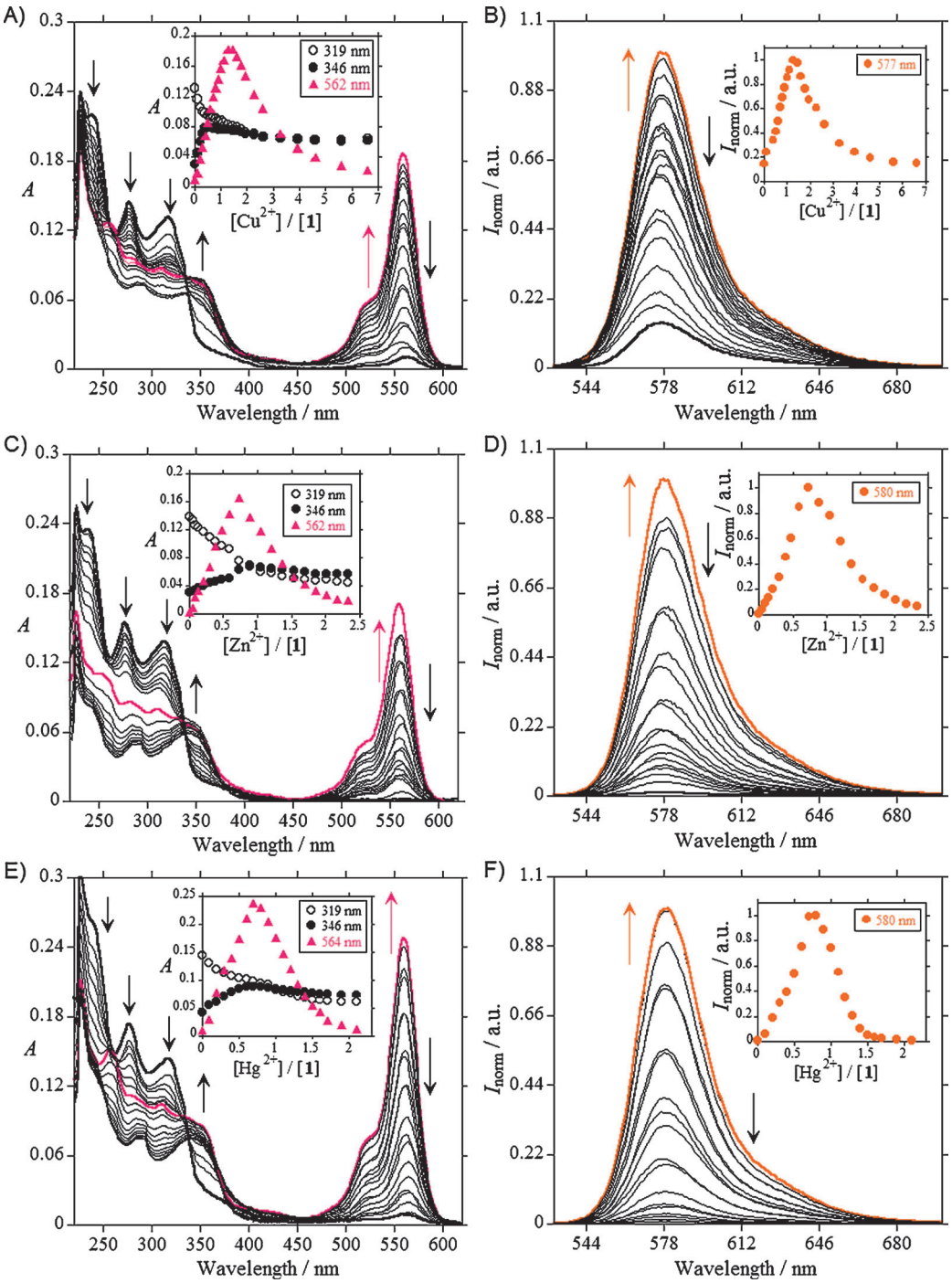

Figure 1. A,C,E) Spectrophotometric and B,D,F) spectrofluorimetric titrations of molecular probe **1** in CH_2Cl_2 as a function of added Cu^{2+} (A,B), Zn^{2+} (C,D), and Hg^{2+} (E,F) in CH_3CN at 298 K. Insets show the absorption at 319, 346, and ~562 nm (A,C,E) and the normalized fluorescence intensity at ~580 nm (B,D,F) ([**1**] = 5.00×10^{-6} M, λ_{exc1} = 520 nm).

crease in the absorption and fluorescence emission responses and a visual color change from pink (visible response) and/or orange (fluorescence response) to colorless (see Figure 3). Nevertheless, Hg^{+} and Cd^{2+} metal ions interact with compound **1** by coordination with the delocalized amide unit, and the addition of increased amounts of these ions did not promote the migration of the metal from this side to the bipyiridine unit. Consequently, the loss of color did not take place (see Figure 3).

The stability constants of the species formed by the interaction of molecular probe **1** in the presence of all metal ions explored were calculated using HypSpec software (Version 1.1) and are summarized in Table 1.[14] All data fit to a 1:1 ligand-to-metal stoichiometry, confirming the Job's plot experiments. Taking into account these values, the sequence of the strongest interaction expected for compound **1** decreases in the following order: $Hg^{+} > Cd^{2+} > Hg^{2+} > Cu^{2+} > Zn^{2+}$, being higher for both metals for which the migration was not observed.

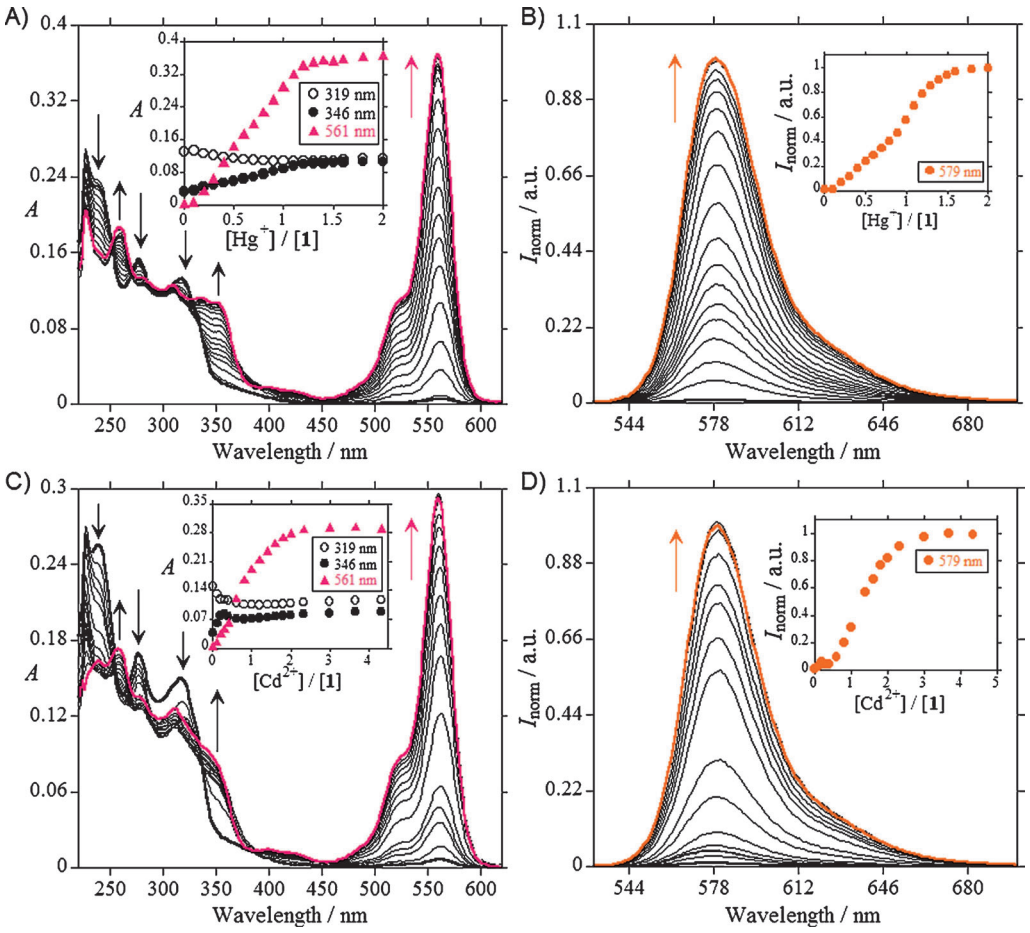

Figure 2. A,C) Spectrophotometric and B,D) spectrofluorimetric titrations of molecular probe **1** in CH_2Cl_2 as a function of added Hg^+ (A, B) and Cd^{2+} (C, D) in CH_3CN at 298 K. Insets show the absorption at 319, 346, and 561 nm (A, C) and the normalized fluorescence intensity at 579 nm (B, D) ([**1**] = 5.00×10^{-6} M, λ_{exc1} = 520 nm).

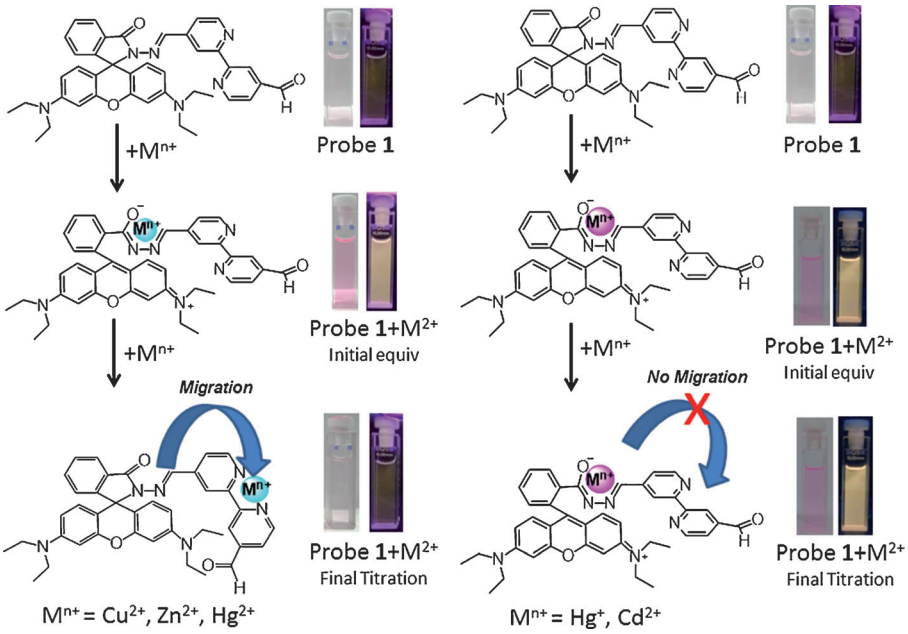

Figure 3. Proposed mechanism of "*migration*" in system **1** for Cu^{2+}, Zn^{2+}, and Hg^{2+} (left) and "*no migration*" for Hg^+ and Cd^{2+} (right). Also shown are images of the solution of **1** in CH_2Cl_2 before and after addition of M^{n+} (for M^{n+} = Cu^{2+}, Zn^{2+}, Hg^{2+}, Hg^+, and Cd^{2+}) under visible light and after excitation at 365 nm using a fluorescence lamp.

Logic operation

To explore the application of compound **1** as a logic gate molecular system based on its complex formation reactions toward Cu^{2+} (Figure 1 A,B), Zn^{2+} (Figure 1 C,D), and Hg^+ (Figure 2 A,B), binary reactions to detect Cu^{2+} (Figure 4) and Zn^{2+} (Figure 5) after the addition of Hg^+ were also carried out. A XOR logic operation can be mimicked with compound **1**[15] using Hg^+ and Cu^{2+} as the two logic inputs, with the normalized emission intensity at 580 nm ($I_{580\,nm}$) as the logic output. The absorption and emission spectra of **1** in dichloromethane solution in the presence of Hg^+ and/or Cu^{2+} are shown in Figure 4.

Table 1. Stability constants for probe **1** in CH_2Cl_2 in the presence of metal ions Cu^{2+}, Zn^{2+}, Hg^{2+}, Hg^{+}, and Cd^{2+} in CH_3CN for a 1:1 metal-to-probe **1** interaction.

M^{n+}	Σ log β [Abs] [Emission]	Σ log β [Emiss] [Emission]
Cu^{2+}	10.38 ($\pm 9.81\times10^{-3}$)	10.32 ($\pm 1.35\times10^{-2}$)
Zn^{2+}	10.29 ($\pm 4.33\times10^{-3}$)	10.14 ($\pm 1.90\times10^{-2}$)
Cd^{2+}	14.13 ($\pm 1.04\times10^{-3}$)	14.37 ($\pm 1.86\times10^{-2}$)
Hg^{2+}	11.09 ($\pm 8.70\times10^{-3}$)	11.29 ($\pm 1.70\times10^{-3}$)
Hg^{+}	15.92 ($\pm 1.58\times10^{-3}$)	16.89 ($\pm 1.67\times10^{-2}$)

[a] Data represent the mean of $n=3$ experiments; SD are given in parentheses.

We define state "1" as the output of $I_{580\ nm} > 0.5$ and state "0" as the output of $I_{580\ nm} < 0.5$. In the absence of the two inputs of Hg^{+} and Cu^{2+} (namely the input combination of "0,0"), the output of $I_{580\ nm}$ is <0.5, corresponding to the "0" state. Upon individual presence of Hg^{+} or Cu^{2+} (namely the input combination of "0,1" or "1,0"), the output of $I_{580\ nm}$ is >0.5. The simultaneous presence of Hg^{+} and Cu^{2+} (namely the input combination of "1,1") can give a low output of $I_{580\ nm}$, showing the "0" state. However, as shown in Figure 5 B, the simultaneous presence of Hg^{+} and Zn^{2+} (namely the input combination of "1,1") can give a high output of $I_{580\ nm}$, showing the "1" state. The above results give a typical truth table for an XOR and OR logic circuits, respectively (Figure 6).[15]

Theoretical calculations

To gain insight into the atomistic details of the coordination modes of the cations to the rhodamine-based receptor, some DFT calculations were performed at the B3LYP/LANL2DZ level using Gaussian 09.[16] In some cases, it was necessary to introduce water molecules to complete the coordination sphere of the metals, such that the calculated association energies fully reflect the preferences of the metals to the distinct receptor binding sites.

Figure 7 shows the lowest-energy gas-phase conformation of the free receptor **1**. This conformation presents the bipyridine fragment twisted around the inter-ring bond such that the nitrogen atoms therein point in opposite directions to minimize the electrostatic interaction between them. The central five-membered ring is closed, leading the spiro center to enable an orthogonal disposition between the bipyridine and rhodamine fragments.

Upon complexation with the cations, the lowest-energy conformations of the resulting mono-complexes present the central five-membered ring opened, allowing the hydrazide nitrogen atoms to be exposed and coordinate the cation (Figure 8) via the electron lone pairs, made available upon opening of the spirolactam ring. Stabilization of the complexes requires water molecules around the cation, both to shield its positive charge and to complete its coordination sphere. In the experimental setup, these water molecules are residually present in the non-coordinating solvent used in the titrations (CH_2Cl_2).

Looking into the coordination mode of Hg^{2+} to **1** (similar discussion is possible for Zn^{2+} and Cu^{2+}), the cation coordinates both hydrazide nitrogen atoms and four water molecules, leading to N···Hg^{2+} distances of 1.95 and 1.98 Å, and H_2O···Hg^{2+} distances between 2.43 and 2.66 Å. This conformation presents the bipyridyl fragment rotated around the bipyridyl–hydrazide bond such that one of the nitrogen atoms from the former fragment is also able to simultaneously establish a hydrogen bond with one of the coordinated water molecules. This type of conformation contrasts with the lowest-energy conformations obtained for the complexation with Cd^{2+} and Hg^{+} (see Figure 8, bottom row, for **1**·Hg^{2+}), in which the bipyridyl fragment does not rotate around the bipyridyl–hydrazide bond, and therefore does not interact with the coordination waters around the metal. Nevertheless, the coordination of the

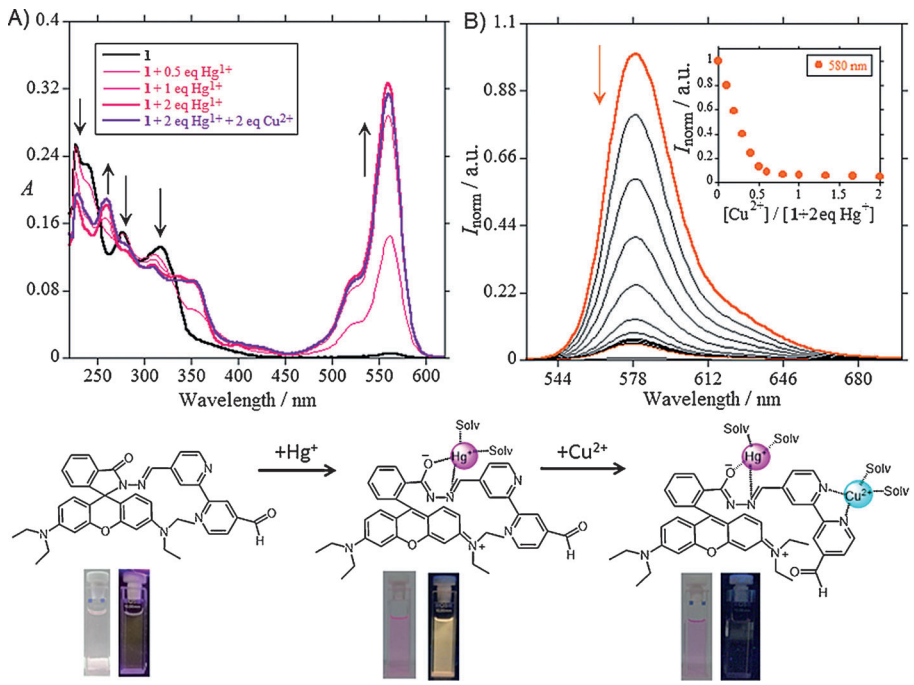

Figure 4. *Top*: A) Spectrophotometric and B) spectrofluorimetric response of **1**–Hg^{+} in CH_2Cl_2 as a function of added Cu^{2+} in CH_3CN at 298 K; inset shows the normalized fluorescence intensity at 580 nm (B) ([**1**] = 5.00×10^{-6} M, λ_{exc1} = 520 nm). *Bottom*: Schematic representation of the proposed interaction of compound **1** with Hg^{+} and Cu^{2+}. Images show the solution of **1** in CH_2Cl_2 before and after the addition of Hg^{+} and Cu^{2+} under visible light and after excitation at 365 nm using a fluorescence lamp.

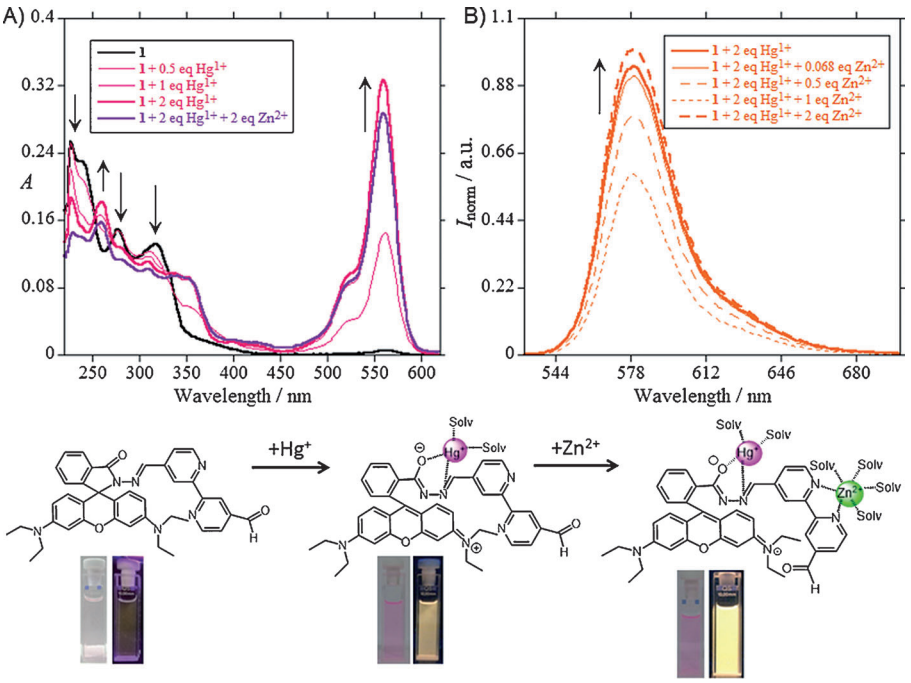

Figure 5. *Top*: A) Spectrophotometric and B) spectrofluorimetric response of **1**–Hg^{+} in CH_2Cl_2 as a function of added Zn^{2+} in CH_3CN at 298 K ([**1**] = 5.00×10^{-6} M, λ_{exc1} = 520 nm). *Bottom*: Schematic representation of the proposed interaction of compound **1** with Hg^{+} and Zn^{2+}. Images show the solution of **1** in CH_2Cl_2 before and after the addition of Hg^{+} and Zn^{2+} under visible light and after excitation at 365 nm using a fluorescence lamp.

Input data			Output data [$I_{580\ nm}$]	
I_1 [Cu^{2+}]	I_2 [Hg^{+}]	I_3 [Zn^{2+}]	O_1	O_2
0	0	0	0	0
0	1	0	1	0
1	0	0	1	0
1	1	0	0	0
0	0	0	0	0
0	1	0	0	1
0	0	1	0	1
0	1	1	0	1

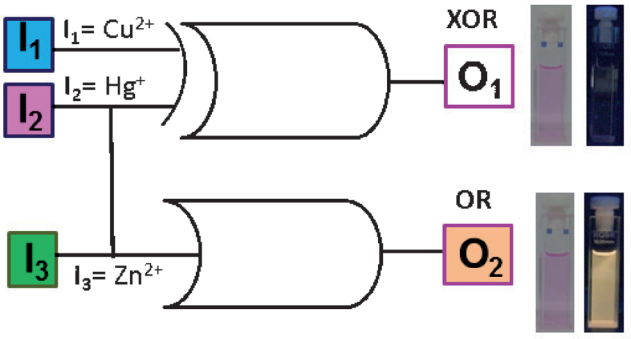

Figure 6. Output response ($I_{580\ nm}$) of compound **1** in CH_2Cl_2 solution ([**1**] = 5.00×10^{-6} M, λ_{exc1} = 520 nm) upon the presence of Cu^{2+} (I_1) and/or Hg^{+} (I_2) corresponding to an XOR logic gate (O_1) and upon the presence of Hg^{+} (I_2) and/or Zn^{2+} (I_3) corresponding to an OR logic gate (O_2).

metal occurs preferentially to the hydrazide nitrogen atoms in a manner similar to that previously described. The direct interaction of the bipyridyl moiety with the hydration waters might provide a direct path to the "cation migration" phenomena observed experimentally upon addition of higher amounts of Cu^{2+}, Zn^{2+}, or Hg^{2+}, but not observed for Cd^{2+} or Hg^{+}. The bipyridyl fragment offers an additional coordination site that can be easily occupied by the cation, although the resulting binding arrangement is slightly less favorable than the former one for all complexes.

The addition of a second cation leads to coordination of the two species to both binding sites of **1**. Figure 8 (top row) presents the lowest-energy conformation of the association of 2 Hg^{2+} and Hg^{2+} and Zn^{2+} to **1**. Similarly to the 1:1 (M/L) complexes described above, the central five-membered ring is opened, leaving the two hydrazide nitrogen atoms available for coordination with the Hg^{2+} cation. In this case, however, the bipyridyl moiety directs its nitrogen atoms in the same direction, coordinating the either the second Hg^{2+} or the Zn^{2+} cation. In both cases, the cations are surrounded by water molecules, thus completing the coordination sphere of the metals.

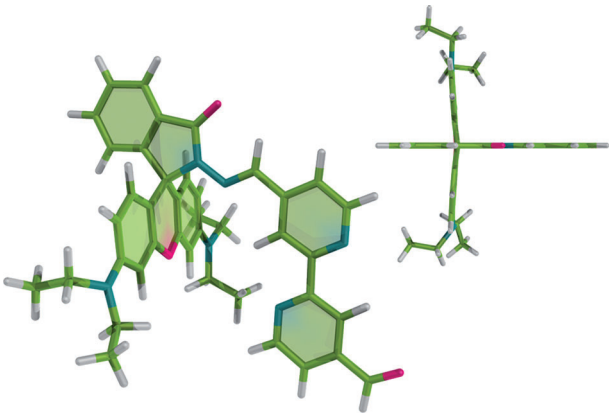

Figure 7. Lowest-energy gas-phase conformation of receptor **1** at the B3LYP/LANLD2Z level. The inset provides a top view of the conformation in which the orthogonal arrangement of the bipyridyl fragment relative to the rhodamine core is visible. Green: carbon, deep teal: nitrogen, hot pink: oxygen, white: hydrogen.

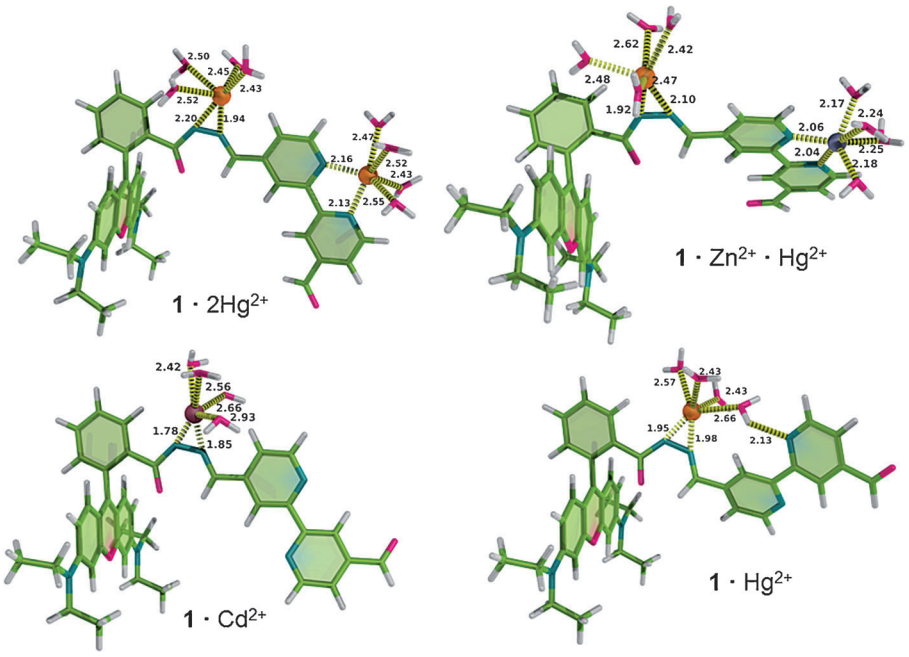

Figure 8. Lowest-energy co-conformations of the association of Cd^{2+} and Hg^{2+} (bottom row) and $2\,Hg^{2+}$ and Zn^{2+}/Hg^{2+} (top row) to receptor **1**, highlighting the interaction with the water molecules that complete the coordination spheres of the metals. Details as in Figure 7 (metals shown as spheres).

Conclusions

In summary, a simple and easy-to-prepare rhodamine B based molecular probe that contains a bipyridyl unit was designed, synthesized, and structurally characterized. Colorimetric and fluorescent responses of the type "off-on-off" were observed upon the addition of Cu^{2+}, Zn^{2+}, and Hg^{2+}. However, an "off-on" response was detected in the presence of Hg^{+} and Cd^{2+}. These results suggested that all metal ions initially interacted with molecular probe **1** by coordination with the delocalized amide unit, which resulted in an increase in the absorption and fluorescence emission response. Nevertheless, Cu^{2+}, Zn^{2+}, and Hg^{2+} metal ions migrated from the amide to the bipyridine framework, yielding a decrease in the absorption and fluorescence emission responses and a visual color change from pink (visible response) and/or orange (fluorescence response) to colorless. In all cases, a 1:1 ligand-to-metal stoichiometry was determined.

DFT calculations were used to test these experimental data. The lowest-energy conformations for the coordination mode of all explored metal ions to **1** suggested that each cation coordinates both hydrazide nitrogen atoms and water molecules. In the case of Cu^{2+}, Zn^{2+}, and Hg^{2+}, this conformation presents the bipyridyl fragment rotated around the bipyridyl–hydrazide bond such that one of the nitrogen atoms from the former fragment is also able to simultaneously establish a hydrogen bond with one of the coordinated water molecules. However, in the presence of Cd^{2+} or Hg^{+} this interaction was not observed to take place. The hydrogen bond interaction could be responsible for providing a direct path to the "cation migration" phenomena observed experimentally upon addition of higher amounts of Cu^{2+}, Zn^{2+}, or Hg^{2+}, but it did not take place with Cd^{2+} or Hg^{+}.

The presence of two binding sites in the molecular probe **1** was exploited to mimic XOR and OR logic operations, using Hg^{+}/Cu^{2+} and Hg^{+}/Zn^{2+} as logic inputs, respectively, and $I_{580\,nm}$ as the logic output.

Experimental Section

Materials and methods

Elemental analyses were performed in a Fisons EA-1108 analyzer at the CACTI, University of Vigo Elemental analysis Service. ^{1}H, ^{13}C, COSY, DEPT, and HSQC NMR spectra were recorded on a Bruker AMX-500 spectrometer (at REQUIMTE, FCT-UNL), and [D_6]DMSO was used as the solvent in all cases. MALDI-ToF MS analyses were performed at the PROTEOMASS-BIOSCOPE Group, using a Bruker MALDI-ToF MS model Ultraflex II Workstation (Bruker, Germany) equipped with a nitrogen laser radiating at 337 nm. The spectra represent accumulations of 5×100 laser shots. The reflector mode was used. The ion source and flight tube pressures were $<1.80\times10^{-7}$ and $<5.60\times10^{-7}$ Torr, respectively. The MALDI MS data of probe **1** (1 or 2 mg mL^{-1}) were recorded using the conventional simple preparation methods, with CH_2Cl_2 as solvent in the absence of MALDI matrix.

Spectrophotometric and spectrofluorimetric measurements

Absorption spectra were recorded on a JASCO V-650 spectrophotometer, and fluorescence emission spectra were recorded on a Horiba JY Scientific Fluoromax 4 spectrofluorimeter. The linearity of fluorescence emission versus concentration was checked in the concentration range used (10^{-4}–10^{-6} M). Correction of the absorbed light was performed when considered necessary. The spectrophotometric characterization and titrations were performed by preparing stock solutions of compounds **1** in CH_2Cl_2 ($\sim10^{-3}$ M) in a 10 mL volumetric flask. The studied solutions were prepared by appropriate dilution of the stock solutions up to 10^{-5}–10^{-6} M. Titrations of probe **1** were carried out by the addition of microliter amounts of standard solutions of the metal ions in CH_3CN. All measurements were performed at 298 K. Fluorescence quantum yields of **1** were measured by using a solution of rhodamine 101 in absolute EtOH (0.01 % HCl) as standard ($[\Phi]=0.54$),[17] and all values were corrected taking the solvent refraction index into account.

DFT calculations

DFT calculations were performed with Gaussian 09[16] with default grids and convergence criteria, using the B3LYP functional and the LanL2DZ basis set, consisting of a D95V set for hydrogen and first-row elements, and a Los Alamos effective core potential (ECP) plus

a DZ set for the valence electrons of the metals.[18] In some cases, it was necessary to introduce water molecules to complete the coordination sphere of the metals, such that the calculated association energies fully reflect the preferences of the metals for the distinct receptor binding sites.

Chemicals and starting materials

Hydrazine hydrate, 2,2′-bipyridine-4,4′-dicarboxaldehyde, and hydrated tetrafluoroborate salts were commercially available (Alfa Aesar and Aldrich). Rhodamine B was purchased from Exciton (USA). The used solvents were of reagent grade and were purified by standard methods.

Synthesis of compound 1

Rhodamine B hydrazide was prepared following a published method.[19] Rhodamine B hydrazide (456 mg, 1.00 mmol) was dissolved in absolute EtOH (25 mL); 2,2′-bipyridine-4,4′-dicarboxaldehyde (112 mg, 0.50 mmol) in THF (25 mL) was then added. The reaction mixture was stirred and heated at reflux for 2 h, after which time it was cooled and filtered. The residue was washed thoroughly with a mixture of cool absolute EtOH and THF (50:50) and dried to afford **1** as a white solid: 280 mg (86%; the yield was calculated based on starting reagents). All product was purified by precipitation. ^{1}H NMR ($CDCl_3$): $\delta = 1.15$ (t, $J = 7.1$ Hz, 12H, NCH_2CH_3), 3.33 (q, $J = 7.1$ Hz, 8H, NCH_2CH_3), 6.31 (dd, $J_1 = 8.9$ Hz, $J_2 = 2.2$ Hz, 2H, Xanthene-H), 6.43 (d, $J = 2.2$ Hz, 2H, Xanthene-H), 6.50 (d, $J = 8.9$ Hz, 2H, Xanthene-H), 7.13 (d, 1H, Ar-H), 7.42 (m, 2H, Ar-H), 7.62 (dd, 2H, Py-H), 7.73 (dd, 2H, Py-H), 7.98 (d, 1H, Ar-H), 8.43 (s, 2H, Py-H), 8.79 (br s, 1H, N=C–H), 10.20 ppm (s, 1H, O=C–H); MALDI-ToF MS: found: $m/z = 651.93$ [**1** + H], calcd for $C_{40}H_{38}N_6O_3 = 650.3$; Elemental analysis (%): found: C 71.63, H 6.27, N 12.38, calcd: C 71.84, H 6.03, N 12.57.

Acknowledgements

S.M.S., E.O., and H.M.S. thank the FCT-MCTES (Portugal) for their postdoctoral grants SFRH/BPD/64752/2009, SFRH/BPD/72557/2010 and SRFH/BPD/73997/2010, respectively. The authors thank the Scientific Association PROTEOMASS (Portugal) for financial support. C.N. thanks the Xunta de Galicia (Spain) for her postdoctoral contract (I2C program). C.L. and J.L.C. thank REQUIMTE-FCT PEst-C/EQB/LA0006/2013 for funding, and the NMR service from the National NMR Facility, supported by Fundação para a Ciência e a Tecnologia (RECI/BBB-BQB/0230/2012).

Keywords: bipyridyls · DFT · logic gates · metals · migration · rhodamine B

[1] a) J. S. Kim, D. T. Quang, *Chem. Rev.* **2007**, *107*, 3780; b) A. T. Wright, E. V. Anslyn, *Chem. Soc. Rev.* **2006**, *35*, 14; c) J. Yoon, S. K. Kim, N. J. Singh, K. S. Kim, *Chem. Soc. Rev.* **2006**, *35*, 355; d) P. A. Gale, *Acc. Chem. Res.* **2006**, *39*, 465; e) T. Gunnlaugsson, M. Glynn, G. M. Tocci, P. E. Kruger, F. M. Pfeffer, *Coord. Chem. Rev.* **2006**, *250*, 3094; f) J. Zhao, M. G. Davidson, M. F. Mahon, G. Kociok-Köhn, T. D. James, *J. Am. Chem. Soc.* **2004**, *126*, 16179; g) R. Martínez-Máñez, F. Sancenón, *Chem. Rev.* **2003**, *103*, 4419; h) J. L. Sessler, D. Seidel, *Angew. Chem. Int. Ed.* **2003**, *42*, 5134; *Angew. Chem.* **2003**, *115*, 5292; i) P. D. Beer, P. A. Gale, *Angew. Chem. Int. Ed.* **2001**, *40*, 486; *Angew. Chem.* **2001**, *113*, 502; j) A. W. Czarnik, *Acc. Chem. Res.* **1994**, *27*, 302.

[2] a) T. Chen, W. Zhu, Y. Xu, S. Zhang, X. Zhang, X. Qian, *Dalton Trans.* **2010**, *39*, 1316; b) M.-L. Ho, K.-Y. Chen, G.-H. Lee, Y.-C. Chen, C.-C. Wang, J.-F. Lee, *Inorg. Chem.* **2009**, *48*, 10304; c) W. Huang, P. Zhou, W. Yan, C. He, L. Xiong, F. Li, C. Duan, *J. Environ. Monit.* **2009**, *11*, 330.

[3] U. Pischel, *Angew. Chem. Int. Ed.* **2007**, *46*, 4026; *Angew. Chem.* **2007**, *119*, 4100.

[4] P. Ball, *Nature* **2000**, *406*, 118.

[5] a) A. P. de Silva, H. Q. N. Gunaratne, C. P. McCoy, *Nature* **1993**, *364*, 42; b) A. P. de Silva, *J. Phys. Chem. Lett.* **2011**, *2*, 2865; c) A. J. Bard, *Integrated Chemical Systems: A Chemical Approach to Nanotechnology*, Wiley, New York, **1994**.

[6] a) L. M. Adleman, *Science* **1994**, *266*, 1021; b) A. P. de Silva, N. D. McClenaghan, *Chem. Eur. J.* **2004**, *10*, 574; c) T. H. Lee, J. I. González, J. Zheng, R. M. Dickson, *Acc. Chem. Res.* **2005**, *38*, 534.

[7] a) Z. Q. Guo, W. H. Zhu, L. J. Shen, H. Tian, *Angew. Chem. Int. Ed.* **2007**, *46*, 5649 – 5653; *Angew. Chem.* **2007**, *119*, 5645; b) A. Petitjean, N. Kyritsakas, J. M. Lehn, *Chem. Eur. J.* **2005**, *11*, 6818; c) K. Rurack, A. Kovalchuck, J. L. Bricks, J. L. Slominskii, *J. Am. Chem. Soc.* **2001**, *123*, 6205.

[8] a) P. A. Vigato, S. Tamburini, L. Bertolo, *Coord. Chem. Rev.* **2007**, *251*, 1311; b) W. Barros, Jr., M. Engelsberg, *Phys. Rev. E* **2003**, *67*, 021905.

[9] P. Mahato, S. Saha, A. Das, *J. Phys. Chem. C* **2012**, *116*, 17448.

[10] Y.-K. Yang, K.-J. Yook, J. Tae, *J. Am. Chem. Soc.* **2005**, *127*, 16760.

[11] a) S. Saha, P. Mahato, M. Baidya, S. K. Ghosh, A. Das, *Chem. Commun.* **2012**, *48*, 9293; b) S. Saha, M. U. Chhatbar, P. Mahato, L. Praveen, A. K. Siddhanta, A. Das, *Chem. Commun.* **2012**, *48*, 1659; c) P. Mahato, S. Saha, E. Suresh, R. Di Liddo, P. P. Parnigotto, M. T. Conconi, M. K. Kesharwani, B. Ganguly, A. Das, *Inorg. Chem.* **2012**, *51*, 1769; d) M. Suresh, A. Shrivastav, S. Mishra, E. Suresh, A. Das, *Org. Lett.* **2008**, *10*, 3013; e) M. Suresh, S. Mishra, S. K. Mishra, E. Suresh, A. K. Mandal, A. Shrivastav, A. Das, *Org. Lett.* **2009**, *11*, 2740; f) C. Núñez, M. Diniz, A. A. Dos Santos, J. L. Capelo, C. Lodeiro, *Dyes Pigm.* **2014**, *101*, 156.

[12] a) C. Lodeiro, J. L. Capelo, J. C. Mejuto, E. Oliveira, H. M. Santos, B. Pedras, C. Núñez, *Chem. Soc. Rev.* **2010**, *39*, 2948; b) N. M. M. Moura, C. Núñez, S. M. Santos, M. A. F. Faustino, J. A. S. Cavaleiro, M. G. P. M. S. Neves, J. L. Capelo, C. Lodeiro, *Inorg. Chem.* **2014**, *53*, 6149; c) N. M. M. Moura, C. Núñez, M. A. F. Faustino, J. A. S. Cavaleiro, M. G. P. M. S. Neves, J. L. Capelo, C. Lodeiro, *J. Mater. Chem. C* **2014**, *2*, 4772; d) N. M. M. Moura, C. Núñez, S. M. Santos, M. A. F. Faustino, J. A. S. Cavaleiro, F. A. Almeida Paz, M. G. P. M. S. Neves, J. L. Capelo, C. Lodeiro, *Chem. Eur. J.* **2014**, *20*, 6684; e) C. Núñez, E. Oliveira, J. García-Pardo, M. Diniz, J. Lorenzo, J. L. Capelo, C. Lodeiro, *J. Inorg. Biochem.* **2014**, *137*, 115; f) E. Oliveira, C. Núñez, B. Rodríguez-González, J. L. Capelo, C. Lodeiro, *Inorg. Chem.* **2011**, *50*, 8797; g) J. Fernández-Lodeiro, C. Núñez, R. Carreira, H. M. Santos, C. Silva López, J. C. Mejuto, J. L. Capelo, C. Lodeiro, *Tetrahedron* **2011**, *67*, 326; h) L. Fernandes, M. Boucher, J. Fernández-Lodeiro, E. Oliveira, C. Nuñez, H. M. Santos, J. L. Capelo, O. N. Faza, E. Bértolo, C. Lodeiro, *Inorg. Chem. Commun.* **2009**, *12*, 905; i) A. Aldrey, C. Núñez, V. García, R. Bastida, C. Lodeiro, A. Macías, *Tetrahedron* **2010**, *66*, 9223; j) A. Aldrey, V. García, C. Lodeiro, A. Macías, P. Pérez-Lourido, L. Valencia, R. Bastida, C. Núñez, *Tetrahedron* **2013**, *69*, 4578.

[13] M. Beija, C. A. M. Afonso, J. M. G. Martinho, *Chem. Soc. Rev.* **2009**, *38*, 2410.

[14] P. Gans, A. Sabatini, A. Vacca, *Talanta* **1996**, *43*, 1739.

[15] N. Wagner, G. Ashkenasy, *Chem. Eur. J.* **2009**, *15*, 1765.

[16] Gaussian 09, Revision A.02, M. J. Frisch, G. W. Trucks, H. B. Schlegel, G. E. Scuseria, M. A. Robb, J. R. Cheeseman, G. Scalmani, V. Barone, B. Mennucci, G. A. Petersson, H. Nakatsuji, M. Caricato, X. Li, H. P. Hratchian, A. F. Izmaylov, J. Bloino, G. Zheng, J. L. Sonnenberg, M. Hada, M. Ehara, K. Toyota, R. Fukuda, J. Hasegawa, M. Ishida, T. Nakajima, Y. Honda, O. Kitao, H. Nakai, T. Vreven, J. A. Montgomery, Jr., J. E. Peralta, F. Ogliaro, M. Bearpark, J. J. Heyd, E. Brothers, K. N. Kudin, V. N. Staroverov, R. Kobayashi, J. Normand, K. Raghavachari, A. Rendell, J. C. Burant, S. Cross, V. Bakken, C. Adamo, J. Jaramillo, R. Gomperts, R. E. Stratmann, O. Yazyev, A. J. Austin, R. Cammi, C. Pomelli, J. W. Ochterski, R. L. Martin, K. Morokuma, V. G. Zakrzewski, G. A. Voth, P. Salvador, J. J. Dannenberg, S. Dapprich, A. D. Daniels, Ö. Farkas, J. B. Foresman, J. V. Ortiz, J. Cioslowski, and D. J. Fox, Gaussian Inc., Wallingford CT (USA), **2009**.

[17] a) J. B. Lambert, E. P. Mazzola, *Nuclear Magnetic Resonance Spectroscopy: an Introduction to Principles, Applications and Experimental Methods*, Prentice Hall, New Jersey, **2004**; b) I. B. Berlman, *Handbook of Fluores-*

cence Spectra of Aromatic Molecules, 2nd ed., Academic Press, New York, **1971**.

[18] a) T. H. Dunning Jr., P. J. Hay in *Modern Theoretical Chemistry, Vol. 3* (Ed.: H. F. Schaefer III), Plenum, New York, **1977**, pp. 1 – 28; b) P. J. Hay, W. R. Wadt, *J. Chem. Phys.* **1985**, *82*, 270; c) W. R. Wadt, P. J. Hay, *J. Chem. Phys.* **1985**, *82*, 284; d) P. J. Hay, W. R. Wadt, *J. Chem. Phys.* **1985**, *82*, 299 – 310.

[19] W. Y. Liu, H. Y. Li, B. X. Zhao, J. Y. Miao, *Org. Biomol. Chem.* **2011**, *9*, 4802.

Received: June 30, 2014
Published online on September 1, 2014